

Accuracy of the Faddeev Random Phase Approximation for Light Atoms

C. Barbieri

Theoretical Nuclear Physics Laboratory, RIKEN Nishina Center, 2-1 Hirosawa, Wako, Saitama 351-0198 Japan

D. Van Neck and M. Degroote

Center for Molecular Modeling, Ghent University, Technologiepark 903, B-9052 Gent, Belgium

(Dated: July 18, 2018)

The accuracy of the Faddeev random phase approximation (FRPA) method is tested by calculating the total and ionization energies of a set of light atoms up to Ar. Comparisons are made with the results of coupled-cluster singles and doubles (CCSD), third-order algebraic diagrammatic construction [ADC(3)], and with the experiment. It is seen that even for two-electron systems, He and Be²⁺, the inclusion of RPA effects leads to satisfactory results and therefore it does not over-correlate the ground state. The FRPA becomes progressively better for larger atomic numbers where it gives ≈ 5 mH more correlation energy and it shifts ionization potentials by 2-10 mH, with respect to its sister method ADC(3). The corrections for ionization potentials consistently reduce the discrepancies with the experiment.

PACS numbers: 31.10.+z, 31.15.Ar

Keywords: Green's function theory; *ab-initio* quantum chemistry; ionization energies

I. INTRODUCTION

Microscopic calculations of many-electron systems are plagued by the exponential increase of degrees of freedom with increasing number of particles. For this reason, *ab-initio* treatments are limited to mid-size molecules with up to ~ 100 electrons [1–3]. On the other hand, the Kohn-Sham formulation [4] of density functional theory (DFT) [5] incorporates many-body correlations (in principle exactly), while only single-particle equations must be solved. Due to this simplicity DFT is the only feasible approach in some modern applications of electronic structure theory. There is therefore a continuing interest in studying conceptual improvements and extensions to the DFT framework [6–9]. Existing DFT functionals can handle short-range inter-electronic correlations quite well, while there is room for improvements in the description of long-range effects [10, 11]. An important issue is how to improve the treatment of long-range (van der Waals) forces and dissociation processes, which could be approached by combining DFT functionals with microscopic calculations in the random phase approximation (RPA) [12–14]. The RPA has also the interesting characteristic that it gives finite correlation energies in metals and the uniform electron gas, where it appropriately screens the Coulomb interaction at large distances [15, 16].

In a recent publication we have considered the *ab-initio* calculation of the Ne atom using Green's function theory in the so called Faddeev-RPA (FRPA) [17]. This approach includes completely two-particle–one-hole (2p1h) and two-hole–one-particle (2h1p) states in the self-energy. Moreover, these configurations are grouped in terms of particle-vibration couplings where the collective vibrations are calculated using RPA. The FRPA was originally proposed for studies of nuclear structure [18–22], however, due to these characteristics it appears capable of treating long-range correlations in both finite and extended electron systems. The present work extends the calculations of Ref. [17] to other closed (sub)shell systems and investigates the accuracy of FRPA for light atoms.

Closely related to this study, is the development of the quasi-particle (QP)-DFT formalism proposed in Ref. [23]. In the QP-DFT the full spectral function is decomposed in the contribution of the QP excitations, in the Landau-Migdal sense [24], and a remainder or background part. Using a functional model for the energy-averaged background part, it is possible to obtain a single-particle self-consistency problem that generates the QP excitations. Such an approach is appealing since it contains the well-developed standard Kohn-Sham formulation of DFT as a special case, while at the same time emphasis is put on the correct description of QPs. Hence, it can provide an improved description of the dynamics at the Fermi surface. Given the close relation between QP-DFT and the Green's function formulation of many-body theory [16, 25], it is natural to employ *ab-initio* calculations in the latter formalism to investigate the structure of possible QP-DFT functionals. In doing so, one wishes to be able to calculate both atomic/molecular systems and the homogeneous electron gas with the same approach.

For QPs associated with outer valence states in molecules, the importance of a treatment that is consistent with at least third-order perturbation theory was already pointed out by Cederbaum and co-workers [26, 27]. Such contributions were then included in the algebraic diagrammatic construction method at third-order [ADC(3)] [28, 29]. The accuracy of the ADC approach has been tested in several studies for both ionization energies (IEs) [30, 31] and excited states [3, 32]. Based on perturbation theory arguments, ADC(3) is expected to be comparable with coupled cluster singles and doubles (CCSD) for correlation energies and with coupled cluster singles doubles and triples (CCSDT) for electron attachment and removal [31]. The ADC(3) approach performs explicit configuration mixing between 2p1h and 2h1p states which generate shake-up configurations of deeply bound orbits. These states are mixed together by ADC(3) theory in a Tamm-Dancoff approximation (TDA) fashion.

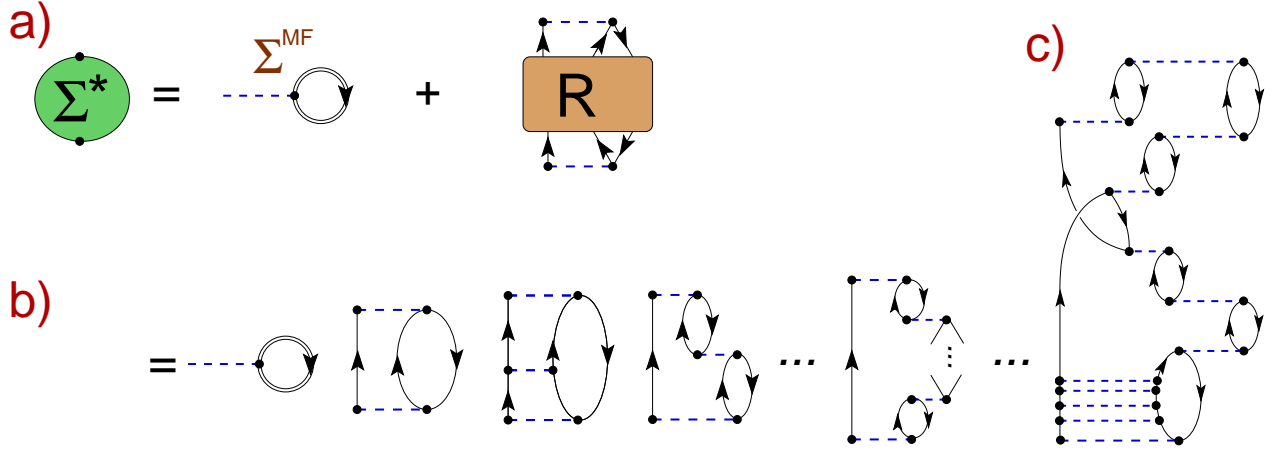


FIG. 1: The self-energy $\Sigma^*(\omega)$ separates exactly into a mean-field term, Σ^{MF} , and the polarization propagator $R(\omega)$ for the 2p1h/2h1p motion, as shown in a). Dashed lines are antisymmetrized Coulomb matrix elements $V_{\alpha\beta,\gamma\delta}$, single lines represent the reference state (a HF propagator), and the double lines represent the correlated propagator of Eq. (1). Upon expansion of $R(\omega)$ in Feynman diagrams, one obtains the series of diagrams b) for the self-energy. The diagram c) is another—more complicated—term appearing in the expansion of $R(\omega)$ that is also included in the FRPA contribution of Fig. 2.

Extended systems require a different approach since the TDA diverges in the particle-hole (ph) channel due to the long-range part of the Coulomb force. In this cases, RPA becomes essential to obtain properly screened interaction and one resorts to the GW method to include the coupling of electrons to ph-RPA phonons [33]. This approach reproduces with high accuracy single-particle levels in solids and atomic systems [34–37] and self-consistent calculations yield the exact correlation energy for the electron gas [38–41]. However, the GW approximation is not free of troubles: while self-consistency improves correlation energies it also deteriorates the description of spectral quantities. The incomplete treatment of Pauli correlations can lead to an incorrect self-screening of the single-particle strength and consequently to poor quasiparticle properties [42]. Deterioration of QP states is also found in atoms when seeking partial improvements of Pauli exchange effects, as in the generalized GW (GGW) [36]. This makes the GW approximation unsatisfactory for atomic and molecular systems. Consistently with these results, Ref. [17] found that including the sole ph-RPA—as done by the GW approximation—exaggerates correlations for outer valence orbitals. To properly compute electron affinities (EAs) and IEs one must also account for interactions in the particle-particle (pp) and hole-hole (hh) channels. When this was done through the FRPA, they corrected large part of the errors of GW and reproduced the correct physics.

The FRPA formulation of Refs. [17, 21] includes the ADC(3) completely and has similar computational requirements. At the same time, the explicit inclusion of RPA introduces the effects of ground state correlations in the phonons' spectra. Thus it holds the promise for bridging calculations of finite and extended electron systems. Still, there remain a number of issues that need to be addressed before this approach can be made useful for electronic structure calculations. First, it is not *a-priori* guaranteed that this approach would behave equally well for few-electron cases: while Pauli correlations are fully included up to 2p1h/2h1p level, the use of RPA still includes violations for more complex excitations. Instabilities and self-screening problems induced by RPA may become more evident in light systems. Second, the inclusion of Pauli exchange at the 2p1h/2h1p introduces technical complications with respect to the standard GW approach and suitable computational schemes will need to be developed for applications to extended systems. This work addresses the first question by applying FRPA to light closed sub-shell atoms.

The essential features of FRPA are reviewed in Sec. II, for the paper to be self-contained. References to the details of the formalism are also given. In our calculations we adopt gaussian basis sets and perform extrapolations to the basis set limit. Hence, we precede the results with a discussion of the accuracy in the extrapolations, in Sec. III A. The results for total energies and IEs are given in Sec. III B and the major conclusions are summarized in Sec. IV.

II. FORMALISM

The theoretical framework of the present study is that of propagator theory. The object of interest is the single-particle propagator [16, 25],

$$g_{\alpha\beta}(\omega) = \sum_n \frac{\langle \Psi_0^N | c_\alpha | \Psi_n^{N+1} \rangle \langle \Psi_n^{N+1} | c_\beta^\dagger | \Psi_0^N \rangle}{\omega - (E_n^{N+1} - E_0^N) + i\eta} + \sum_k \frac{\langle \Psi_0^N | c_\beta^\dagger | \Psi_k^{N-1} \rangle \langle \Psi_k^{N-1} | c_\alpha | \Psi_0^N \rangle}{\omega - (E_0^N - E_k^{N-1}) - i\eta}, \quad (1)$$

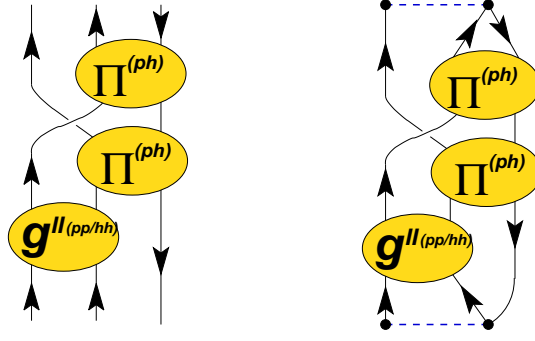


FIG. 2: *Left:* Example of one of the diagrams for $R(\omega)$ that are summed to all orders by means of the FRPA Eqs. (7). Each of the ellipses represent an infinite sum of RPA ladders [$g^{II}(\omega)$] or rings [$\Pi(\omega)$]*—*see Eqs. (4), (5) and Fig. 3. Contributions of all possible partial waves are included. *Right:* The corresponding contribution to the self-energy, obtained upon insertion of $R(\omega)$ into Eq. (3).

where α, β, \dots , label a complete orthonormal basis set and c_α (c_β^\dagger) are the corresponding second quantization destruction (creation) operators. In these definitions, $|\Psi_n^{N+1}\rangle$, $|\Psi_k^{N-1}\rangle$ are the eigenstates, and E_n^{N+1} , E_k^{N-1} the eigenenergies of the $(N \pm 1)$ -electron system. Therefore, the poles of the propagator reflect the EAs and IEs. Eq. (1) also yields the total binding energy via the Migdal-Galitskiĭ-Koltun sum rule [16, 43].

The one-body Green's function is computed by solving the Dyson equation (from hereafter, summations over repeated indices are implied)

$$g_{\alpha\beta}(\omega) = g_{\alpha\beta}^0(\omega) + g_{\alpha\gamma}^0(\omega) \Sigma_{\gamma\delta}^*(\omega) g_{\delta\beta}(\omega) , \quad (2)$$

where $g^0(\omega)$ is the propagator for a free particle (with only kinetic energy). The irreducible self-energy $\Sigma_{\gamma\delta}^*(\omega)$ acts as an effective, energy-dependent, potential that can be written as

$$\begin{aligned} \Sigma_{\alpha\beta}^*(\omega) &= \Sigma_{\alpha\beta}^{MF} + \tilde{\Sigma}_{\alpha\beta}(\omega) \\ &= \int \frac{d\omega}{2\pi i} V_{\alpha\gamma,\beta\delta} g_{\delta\gamma}(\omega) e^{-i\omega\eta^+} + \frac{1}{4} V_{\alpha\lambda,\mu\nu} R_{\mu\nu\lambda,\mu'\nu'\lambda'}(\omega) V_{\mu'\nu',\beta\lambda'} , \end{aligned} \quad (3)$$

where $V_{\alpha\beta,\gamma\delta}$ are antisymmetrized Coulomb matrix elements. In Eq. (3) we have emphasized the mean-field (MF) contribution to the self-energy. This generalizes the Hartree-Fock (HF) potential by replacing the Slater MF with the (correlated) density matrix extracted from the dressed propagator (1). The Σ^{MF} is represented by the first diagram on the right hand side in Figs. 1a) and 1b). The remaining term, $\tilde{\Sigma}(\omega)$, accounts for deviations from the mean-field and depends on the polarization propagator $R(\omega)$ which involves the simultaneous propagation of 2p1h or 2h1p *and higher* excitations. Eq. (3) is represented in Fig.1a) in terms of Feynman diagrams. The polarization propagator $R(\omega)$ can also be expanded in terms of Coulomb matrix elements and simpler propagators, as shown in Figs. 1b) and 1c). This approach also helps in identifying key physics ingredients of the many-body dynamics. By truncating the expansion to a particular subset of diagrams or many-body correlations, one can then construct suitable approximations to the self-energy or seek for systematic improvements of the method. Moreover, since infinite sets of linked diagrams are summed the approach is non-perturbative and satisfies the extensivity condition [2].

In the following we are interested in describing the coupling of single-particle motion to ph, pp and hh collective excitations of the system. Following Ref. [44], we first calculate the corresponding propagators by solving the RPA equations in the ph and pp/hh channels. These are then inserted in the self-energy by solving a set of Faddeev equations to generate the 2p1h and 2h1p components of $R(\omega)$. This approach is thus referred to as Faddeev RPA. The whole procedure is equivalent to regrouping an infinite subset of Feynman diagrams in the expansion of $R(\omega)$ as shown in Fig. 2.

The details of the FRPA approach are given in Refs. [17, 44] and are synthesized in Sec. II A below. For the discussion of the present work, it is sufficient to note that including only ph propagators corresponds to the same physics as the GW approach [33]. The FRPA method goes beyond the GW since it accounts completely for Pauli correlations at the 2p1h/2h1p level and include the propagation of pp/hh configurations. The latter interfere with ph phonons and have important effects for ionization energies in finite systems [17]. Contributions from all channels and in all possible partial waves are included in FRPA, as it is required for a complete solution of the problem. For non-extended systems, it is sometimes possible to use the TDA to calculate collective modes, instead of RPA. It can be show that in this situation the FRPA reduces to the third-order ADC of Schirmer [29]. In the following we will refer equivalently to this approximation as either FDTA or ADC(3). Throughout this paper, the dynamic self-energy $\tilde{\Sigma}(\omega)$ is calculated in terms of a HF reference state, while Σ^{MF} is derived self-consistently from the dressed propagator, by iterating Eqs. (2) and (3).

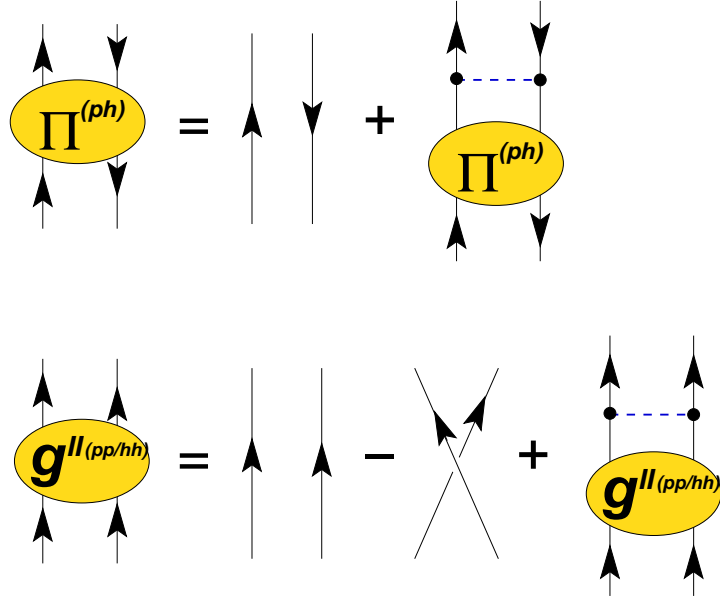


FIG. 3: Diagrammatic equations for the polarization (above) and the two-particle (below) propagators. All time orderings are included in order to generate the RPA series.

A. The Faddeev random phase approximation method

Following Refs. [17, 44], we first consider the ph polarization propagator that describes excited states of the N -electron system

$$\begin{aligned} \Pi_{\alpha\beta,\gamma\delta}(\omega) &= \sum_{n \neq 0} \frac{\langle \Psi_0^N | c_\beta^\dagger c_\alpha | \Psi_n^N \rangle \langle \Psi_n^N | c_\gamma^\dagger c_\delta | \Psi_0^N \rangle}{\omega - (E_n^N - E_0^N) + i\eta} \\ &\quad - \sum_{n \neq 0} \frac{\langle \Psi_0^N | c_\gamma^\dagger c_\delta | \Psi_n^N \rangle \langle \Psi_n^N | c_\beta^\dagger c_\alpha | \Psi_0^N \rangle}{\omega + (E_n^N - E_0^N) - i\eta}, \end{aligned} \quad (4)$$

and the two-particle propagator that describes the addition/removal of two electrons

$$\begin{aligned} g_{\alpha\beta,\gamma\delta}^{II}(\omega) &= \sum_n \frac{\langle \Psi_0^N | c_\beta c_\alpha | \Psi_n^{N+2} \rangle \langle \Psi_n^{N+2} | c_\gamma^\dagger c_\delta^\dagger | \Psi_0^N \rangle}{\omega - (E_n^{N+2} - E_0^N) + i\eta} \\ &\quad - \sum_k \frac{\langle \Psi_0^N | c_\gamma^\dagger c_\delta^\dagger | \Psi_k^{N-2} \rangle \langle \Psi_k^{N-2} | c_\beta c_\alpha | \Psi_0^N \rangle}{\omega - (E_0^N - E_k^{N-2}) - i\eta}. \end{aligned} \quad (5)$$

These Green's functions contain in their Lehmann representations all the relevant information regarding the excitation of ph and pp or hh modes. In this work we are interested in studying the influence of collective vibrations, which can be described within the RPA. The propagators of Eqs. (4) and (5) are then evaluated by solving the usual RPA equations, which are depicted diagrammatically in Fig. 3. In order to fulfill Pauli constraints in the expansion for $R(\omega)$ one must employ the generalized version of RPA, in which the Coulomb matrix elements are the antisymmetrized ones. Since these equations reflect two-body correlations, they still have to be coupled to an additional single-particle propagator, as in Fig. 2, to obtain the corresponding approximation for the 2p1h and 2h1p components of $R(\omega)$. This is achieved by solving two separate sets of Faddeev equations, as discussed in Ref. [44].

The $R(\omega)$ contains two separate terms that propagate either 2p1h or 2h1p states. Taking the 2p1h case as an example, one can further split $R^{(2p1h)}(\omega)$ again in three different components $\bar{R}^{(i)}(\omega)$ ($i = 1, 2, 3$) that differ from each other by the last pair of lines that interact in their diagrammatic expansion,

$$\bar{R}_{\alpha\beta\gamma,\mu\nu\lambda}^{(2p1h)}(\omega) = \left[G_{\alpha\beta\gamma,\mu\nu\lambda}^{0>}(\omega) - G_{\beta\alpha\gamma,\mu\nu\lambda}^{0>}(\omega) \right] + \sum_{i=1,2,3} \bar{R}_{\alpha\beta\gamma,\mu\nu\lambda}^{(i)}(\omega), \quad (6)$$

where $G^{0>}(\omega)$ is the 2p1h propagator for three non-interacting lines. These components are solutions of the following set of Faddeev equations [45]

$$\begin{aligned} \bar{R}_{\alpha\beta\gamma,\mu\nu\lambda}^{(i)}(\omega) &= G_{\alpha\beta\gamma,\mu'\nu'\lambda'}^{0>}(\omega) \Gamma_{\mu'\nu'\lambda',\mu''\nu''\lambda''}^{(i)}(\omega) \\ &\times \left[\bar{R}_{\mu''\nu''\lambda'',\mu\nu\lambda}^{(j)}(\omega) + \bar{R}_{\mu''\nu''\lambda'',\mu\nu\lambda}^{(k)}(\omega) \right. \\ &\left. + G_{\mu''\nu''\lambda'',\mu\nu\lambda}^{0>}(\omega) - G_{\nu''\mu''\lambda'',\mu\nu\lambda}^{0>}(\omega) \right], \quad i = 1, 2, 3, \end{aligned} \quad (7)$$

where (i, j, k) are cyclic permutations of $(1, 2, 3)$. The interaction vertices $\Gamma^{(i)}(\omega)$ contain the couplings of a ph, see Eq. (4), or pp/hh, see Eq. (5), excitation to a freely propagating line. The propagator $R(\omega)$ which we employ in Eq. (3) is finally obtained by

$$R_{\alpha\beta\gamma,\mu\nu\lambda}^{(2p1h)}(\omega) = U_{\alpha\beta\gamma,\mu'\nu'\lambda'} \bar{R}_{\mu'\nu'\lambda',\mu''\nu''\lambda''}^{(2p1h)}(\omega) U_{\mu''\nu''\lambda'',\mu\nu\lambda}^\dagger, \quad (8)$$

where the correction vertex U ensures consistency with perturbation theory up to third order. The explicit formulae for $\Gamma^{(i)}(\omega)$ and U are given in terms of the propagators of Eqs. (4), (5) and the interaction $V_{\alpha\beta,\gamma\delta}$. They are discussed in detail in Ref. [17]. The calculation of the 2h1p component of $R(\omega)$ follows completely analogous steps.

The present formalism includes the effects of ph and pp/hh motion simultaneously, while allowing interferences between these modes. These excitations are evaluated here at the RPA level and are then coupled to each other by solving Eqs. (7). This generates an infinite resummation of diagrams, including the one displayed in Fig. 2. When one uses TDA to approximate phonons this expansion reduces to standard configuration mixing between 2p1h or 2h1p states. As already noted, with the present formulation of Eqs. (6-8) the FTDA turns out to be exactly equivalent to the ADC(3) formalism of Ref. [29].

III. RESULTS

We considered a set of neutral atoms and ions corresponding to closed shell and subshell configurations with $Z \leq 18$. The calculations of the smallest systems (He, Be and Be^{2+}) were performed using the correlation-consistent polarization valence gaussian bases, cc-pvXz, of increasing quality from double- to quintuple-zeta ($X=2-5$). For the larger atoms it was found that a sizable fraction of the correlation energy is lost with similar bases. The remaining systems were therefore calculated with the corresponding core-valence bases, cc-pcvXz, which include additional compact gaussians to improve the description of the core electrons. This choice was seen to speed up the convergence and led to accurate results for these atoms [54]. The correction to the correlation energies induced by the extra core orbits increases with the number of electrons and it was found to be ≈ 40 mH for Ne and ≈ 300 mH for Mg.

The bases for the Be^{2+} (Mg^{2+}) ions were obtained from the cc-p(c)vXz sets for He (Ne) but scaling the corresponding single-particle orbits to correct for the different atomic number,

$$\phi_{\text{Be}^{2+}/\text{Mg}^{2+}}^i(r) \propto \phi_{\text{He/Ne}}^i\left(r \frac{Z}{N}\right) \quad (9)$$

where Z is the nuclear charge and $N=Z-2$ the number of electrons.

Correlation and ionization energies were computed with both the FTDAc/ADC(3)c and the FRPAc methods. In this notation, the letter 'c' indicates the self-consistent treatment of the sole MF diagram in the self-energy [first diagram on the r.h.s. in Figs. 1a) and 1b)]. In other words, Σ^{MF} is renormalized by evaluating it directly in terms of the fully correlated propagator, instead of the reference state. This aspect is important since it consistently includes all the PT contributions up to third-order and more. The ground states energies were also compared to the results of CCSD. In all cases the HF wave functions (calculated for each basis set) were used as the reference state.

A. Convergence

Total binding energies predicted by both Green's function theory and CCSD are shown with the results of full configuration interaction (FCI) in Tab. I. For Ne atom in cc-pcvDz, Green's functions and CCSD agree with each other and deviate from the exact result by less than 2 mH. FRPA gives just a very small correction but it halves the discrepancy between FTDA and FCI. The total correlation energy for this basis is 233 mH. The atom of Be is the most difficult case among those discussed here due to the fact that this is not a good closed-shell system. In this system, a near degeneracy between the 2s and 2p orbitals leads to very soft excitations of the $J^\pi=1^-, S=1$ states and drives the ph-RPA equations close to instability. To avoid this, the FRPA was solved by employing the TDA approximation of the polarization propagator, Eq.(4), in this channel alone (all other partial waves were treated properly in RPA). The resulting correlation energies agree with FTDAc/ADC(3)c, showing that RPA is not crucial for

this small system neither it introduces spuriousities by over-correlating the ground state. FCI calculations of Be were possible for all bases up to quintuple-zeta and are reproduced by CCSD with high accuracy. However, FTDAc/ADC(3)c and FRPAc are consistently behind by about 9 mH, corresponding to 10% of the total correlation energy. This is the most serious discrepancy we obtain in this work and suggest a limitation of the FRPA—in its present form—for near-degenerate systems. To overcome this, it may be necessary to introduce self-consistency in the polarization propagator $R(\omega)$, to account for orbit relaxation, or to improve the treatment of the excitation spectrum of the polarization propagator beyond bare ph states [46] [55]. The close agreement between FTDAc/ADC(3)c and FRPAc in Tab. I is a welcome feature since for a few electrons in the Be atom one should not expect collectivity effects to be important. Although the RPA approximation is not meant for few-body systems, this result (and the one for He, below) shows that it can be safely applied also in this regime without serious consequences. The usual issues of RPA for cases of near degeneracy remain and may lead to instabilities in certain channels, as just described.

Extrapolations to the basis set limit were obtained from two consecutive sets according to

$$E_X = E_\infty + AX^{-3}, \quad (10)$$

where X is the cardinal number of the basis. This relation is known to give proper extrapolations for correlation energies [1]. In Sec. III B, we will apply it to ionization energies as well, remembering that these are also differences between eigenenergies. Table II gives some examples of the calculated binding energies for all bases sizes and shows the convergence of the extrapolated results. In the smallest systems, up to Ne, we find changes of less than 2 mH between the last two extrapolations ($X=T, Q$ and $X=Q, 5$). This number can be taken as a measure of the uncertainty in reaching the basis set limit. For the larger atoms Mg is the one that converges more slowly, with a difference of 10 mH (we found 7 mH for Ar). Calculations with $X=6$ are beyond present computational capabilities. However, given the fast convergence with increasing cardinal number, it appears safe to assume an uncertainty of ≤ 5 mH for these cases.

E_{tot}	Ne		Be		
	cc-pcvDz	cc-pvDz	cc-pvTz	cc-pvQz	cc-pv5z
ADC(3)c/FTDAc	-128.7191	-14.6089	-14.6154	-14.6314	-14.6375
FRPAc	-128.7210	-14.6084	-14.6150	-14.6310	-14.6371
CCSD	-128.7211	-14.6174	-14.6236	-14.6396	-14.6457
full CI	-128.7225	-14.6174	-14.6238	-14.6401	-14.6463

TABLE I: Total binding energies (in Hartrees) for Ne and Be obtained for cc-p(c)vXz bases of different sizes. The results obtained with ADC(3)c and FRPAc (with partial self-consistency in the MF diagram) and with the CCSD methods are compared to FCI calculations.

E_{tot}		cc-p(c)vDz	cc-p(c)vTz	cc-p(c)vQz	cc-p(c)v5z	Experiment
Be:	calc.	-14.6084	-14.6150	-14.6310	-14.6371	-14.6674
	extrap.		-14.6178	-14.6427	-14.6436	
Ne:	calc.	-128.7210	-128.8643	-128.9079	-128.9226	-128.9383
	extrap.		-128.9246	-128.9397	-128.9381	
Mg:	calc.	-199.8147	-199.9507	-200.0033	-200.0271	-200.054
	extrap.		-200.0080	-200.0417	-200.0519	

TABLE II: Convergence of binding energies (in Hartrees) in the FRPAc approach. First lines: total energies calculated in using double ($X=D$) to quintuple ($X=5$) valence orbitals basis sets. Second lines: results extrapolated from two consecutive sets using Eq. (10). The Be atom was calculated with the cc-pvXz bases, while Ne and Mg were done using cc-pcvXz. The experimental energies are from Refs. [48, 49].

B. Ground states and ionization energies of simple atoms

Table III shows the ground state energies extrapolated from $X=Q, 5$ for both Green's function and CCSD methods. These are compared to the corresponding Hartree-Fock results and the experiment. The empirical values are from Refs. [47–49] and

have been corrected by subtracting relativistic effects. The CCSD results for He and Be²⁺ are equivalent to FCI, from which we see that FRPac misses 1 mH, or 2%, of the correlation energy of He. In larger systems FRPac explains at least 99% of the correlation energies and all calculations, including CCSD, agree with the experiment within the uncertainty expected from basis extrapolation. For $Z \geq 10$, the inclusion of RPA phonons predicts about 5 mH more binding than the corresponding FTDac/ADC(3)c. The atom of Be is the only exception to this trend as already noted above. In this case the 9 mH difference between FRPac and CCSD is seen also in the basis limit. Based on the agreement between FCI and CCSD in Tab.I, the remaining discrepancy with the experiment (≈ 15 mH) may be due the basis set employed which is probably not capable to accommodate the relevant correlation effects. We have attempted FRPac calculations with the aug-cc-pvXz bases which should allow for a better description of the valence orbits but without any appreciable change in the results.

The Ne atom was also computed in the FRPA approach by using a Hartree-Fock basis with a discretized continuum [17]. The size of the basis set was chosen as large as possible to approach the basis set limit, however, the set was optimized for the description of IEs and EAs rather than for treating core orbits. The total binding energy obtained is 128.888 H, away from the basis set limit of Tab. III and the experiment.

	Hartree-Fock	FTDac	FRPac	CCSD	Experiment
He	-2.8617 (+42.0)	-2.9028 (+0.9)	-2.9029 (+0.8)	-2.9039 (-0.2)	-2.9037
Be ²⁺	-13.6117 (+43.9)	-13.6559 (-0.3)	-13.6559 (-0.3)	-13.6561 (-0.5)	-13.6556
Be	-14.5731 (+94.3)	-14.6438 (+23.6)	-14.6436 (+23.8)	-14.6522 (+15.2)	-14.6674
Ne	-128.5505 (+387.8)	-128.9343 (+4.0)	-128.9381 (+0.2)	-128.9353 (+3.0)	-128.9383
Mg ²⁺	-198.83 7 (+444)	-199.226 (-5)	-199.228 (-7)	-199.225 (-4)	-199.221
Mg	-199.616 (+438)	-200.048 (+6)	-200.052 (+2)	-200.050 (+4)	-200.054
Ar	-526.820 (+724)	-527.543 (+1)	-527.548 (-4)	-527.536 (+8)	-527.544
σ_{rms} [mH]	392	9.5 (3.6)	9.5 (3.4)	6.9 (4.2)	

TABLE III: Hartree-Fock, ADC(3)c/FTDac, FRPac and CCSD binding energies (in Hartrees) extrapolated from the cc-p(c)vQz and cc-p(c)v5z basis sets. He, Be²⁺ and Be were calculated with the cc-pvXz bases, while cc-pcvXz bases were used for the remaining atoms. The deviations from the experiment are indicated in parentheses (in mHartrees). The experimental energies are from Refs. [47–49]. The *rms* errors in parentheses are calculated by neglecting the Be results.

Ionization energies are shown in Tab. IV, together with the predictions from Hartree-Fock theory and the second-order self-energy (obtained by retaining only the first two diagrams of Fig. 1b). Second-order corrections account for a large part of correlations but still lead to sizable errors. The additional correlations included in the present calculations appear to reduce this error substantially. The FTDac/ADC(3)c results give a measure of the importance of a treatment that is consistent with at least third order perturbation theory [27]. Corrections are particularly large for states with higher ionization energies where the density of 2h1p states is increased. Since configuration mixing among these states is not introduced by strict second-order perturbation theory, calculations at least at the level of FTDac are required in these cases. Configuration mixing among the 2h1p states reduces the errors in the 1s state in Be by a factor of five. Another effect is the fragmentation of the 3s orbit of Ar. Second-order calculations predict this as a quasiparticle state 36 mH away from the empirical energy that carries 0.81 of the total orbit’s intensity. A small satellite state with relative intensity of 0.10 is calculated at larger separation energies. The mixing with 2h1p configurations corrects the energies of both peaks and redistributes their strengths more correctly. For the FRPac calculation the peak at 1.065 H has intensity of 0.61, close to the experimental value (0.55 found at 1.075 H [50]). The second peak is obtained at 1.544 H and carries the remaining strength of the original quasiparticle.

Adding the effects of collective RPA phonons has a larger impact on ionization than on correlation energies. Almost all the IE calculated shift closer to the experimental values by a few mH. The only exceptions are the two-electron He atom, where the RPA approach may tend to overestimate correlations, and the first ionization of Be, where soft excitations invalidate the RPA. In general, the *rms* error for the valence orbits of Tab. IV lowers from 13.7 to 10.6 mH, passing from FTDac to FRPac.

The FRPac IE of the Ne atom were also computed in the discretized continuum basis of Ref. [17]. The first and second ionization energies obtained are 0.801 and 1.795 H, in good agreement with the extrapolations of Tab. IV. This gives us confidence on applying Eq. (10) also for quasiparticle states.

IV. CONCLUSIONS AND DISCUSSION

In conclusion, we have performed microscopic calculations of total and ionization energies in order to assess the accuracy of the Faddeev RPA approach for light atoms.

		Hartree-Fock	(2 nd order)c	FTDAc/ ADC(3)c	FRPAc	Experiment [51, 52]
He:	1s	0.918 (+14)	0.9012 (-2.5)	0.9025 (-1.2)	0.9008 (-2.9)	0.9037
Be ²⁺ :	1s	5.6672 (+116)	5.6542 (-1.4)	5.6554 (-0.2)	5.6551 (-0.5)	5.6556
Be:	2s	0.3093 (-34)	0.3187 (-23.9)	0.3237 (-18.9)	0.3224 (-20.2)	0.3426
	1s	4.733 (+200)	4.5892 (+56)	4.5439 (+11)	4.5405 (+8)	4.533
Ne:	2p	0.852 (+57)	0.752 (-41)	0.8101 (+17)	0.8037 (+11)	0.793
	1s	1.931 (+149)	1.750 (-39)	1.8057 (+24)	1.7967 (+15)	1.782
Mg ²⁺ :	2p	3.0068 (+56.9)	2.9217 (-28.2)	2.9572 (+7.3)	2.9537 (+3.8)	2.9499
	1s	4.4827	4.3283	4.3632	4.3589	
Mg:	3s	0.253 (-28)	0.267 (-14)	0.272 (-9)	0.280 (-1)	0.281
	2p	2.282 (+162)	2.117 (-3)	2.141 (+21)	2.137 (+17)	2.12
Ar:	3p	0.591 (+12)	0.563 (-16)	0.581 (+2)	0.579 (\approx 0)	0.579
	3s	1.277 (+202)	1.111 (+36)	1.087 (+12)	1.065 (-10)	1.075
	3s		1.840	1.578	1.544	
σ_{rms} [mH]		81.4	29.3	13.7	10.6	

TABLE IV: Ionization energies obtained with Hartree-Fock, second-order perturbation theory for the self-energy, FTDAc and with the full Faddeev-RPAC (in Hartrees). All results are extrapolated from the cc-p(c)vQz and cc-p(c)v5z basis sets (see Table III). The deviations from the experiment (indicated in parentheses) and the *rms* errors are given in mHartrees. The experimental energies are from Ref. [51, 52].

The FRPA method is an expansion of the many-body self-energy that makes explicit the coupling between particles and collective phonons. This formalism includes all contributions from perturbation theory up to third order, which is crucial to a correct prediction of IEs for outer-valence electrons in atomic and molecular systems. At the same time, it also includes full resummations of RPA diagrams necessary to screen the long-range Coulomb interaction in extended systems [15, 16]. While the FRPA includes completely the ADC(3) theory, it is not *a-priori* guaranteed that it performs equally well in small systems since problems related to violations of the Pauli principle—inherent with the RPA method—could worsen in this situation. Nevertheless, the present results show that this is not the case and the approach is capable of good accuracy even for the two-electron problem.

In general, it is found that FTDAc/ADC(3)c and FRPAc give very similar results for the lightest systems while the inclusion of RPA theory for phonons leads to small but systematic improvements as the atomic number increases. For total binding energies, their difference is negligible in the He and Be atoms while the FRPAc yields \approx 5 mH more correlation energy for atomic numbers $Z \geq 10$. Except for the lightest atoms, 99% of the the total correlation energy is normally recovered and the total energies obtained agree well with CCSD (as expected [31]). The discrepancies with the experimental data are also within the errors estimated for the extrapolation to the basis set limit. The only notable exception is the neutral Be atom, for which the small gap at the Fermi surface complicates the extraction of the correlation energy. In this case, the discrepancy obtained with respect to the experiment appears to be mostly due to deficiencies in the basis set. However, a smaller fraction of it is probably related to missing correlations and/or to the lack of full self-consistency in the FRPAc (HF reference states were used).

Similar trends are found for the ionization energies. For the two-electron cases, He and Be²⁺, FRPAc does not introduce improvements with respect to FTDAc/ADC(3)c but still gives sensible predictions. The above problems in describing the correlations of neutral Be are also reflected in the results for the first ionization orbit. For all other cases, the introduction of RPA phonons shifts IEs by 2-10 mH and always brings them closer to the experiment. On average, the *rms* error for outer valence IEs lowers from 13.7 to 10.6 mH. The 3s orbit in Ar is found to be fragmented and configuration mixing effects between 2h1p states are required to obtain the correct ionizaion energy and relative intensity.

Numerically, the FRPA can be implemented as a diagonalization in 2p1h-2h1p space, implying about the same cost as an ADC(3) calculation. The present study was based on numerical codes originally developed in nuclear physics and for spherical systems [18, 44], which are not suitable for chemistry applications. Testing the FRPA approach on molecules requires developing appropriate codes that handle molecular geometries. Work along this line is in progress and will be reported it in a forthcoming

publication [53].

Due to the inclusion of RPA excitations, the FRPA method holds promise of bridging the gap between accurate descriptions of quasiparticles in finite and extended systems. Investigating the feasibility of FRPA for larger molecules and the electron gas is therefore a priority for future research efforts. Consistent calculations of quasiparticle properties in these cases, once feasible, will be important for constraining functionals in quasiparticle density functional theory [23].

Acknowledgments

We acknowledge several useful discussions with Prof. W. H. Dickhoff. This work was supported by the Japanese Ministry of Education, Science and Technology (MEXT) under KAKENHI grant no. 21740213. MD acknowledges support from FWO-Flanders. DVN and MD are members of the QCMM Alliance Ghent-Brussels.

-
- [1] T. Helgaker, *et al.*, *J. Phys. Org. Chem.* **17**, 913 (2004).
 [2] R.J. Bartlett and M. Musiał, *Rev. Mod. Phys.* **79**, 291 (2007).
 [3] J. H. Starcke, M. Wormit, and A. Drew, *J. Chem. Phys.* **130**, 024104 (2009).
 [4] W. Kohn and L. J. Sham, *Phys. Rev.* **140**, A1133 (1965).
 [5] P. Hohenberg and W. Kohn, *Phys. Rev.* **136**, B864 (1964).
 [6] R. J. Bartlett *et al.*, *J. Chem. Phys.* **122**, 034104 (2005); *J. Chem. Phys.* **123**, 062205 (2005).
 [7] P. Mori-Sanchez, Q. Wu, and W. T. Yang, *J. Chem. Phys.* **123**, 062204 (2005).
 [8] A. Pastore, F. Barranco, R. A. Broglia, and E. Vigezzi, *Phys. Rev. C* **78**, 024315 (2008).
 [9] B. Gebremariam, T. Duguet, and S. K. Bogner, [arXiv:0910.4979](https://arxiv.org/abs/0910.4979) [nucl-th].
 [10] Z. Yan, J. P. Perdew, and S. Kurth, *Phys. Rev. B* **61**, 16430 (2000).
 [11] F. Furche, *J. Chem. Phys.* **129**, 114105 (2008).
 [12] J. F. Dobson, in *Topics in Condensed Matter Physics*, ed. M. P. Das (Nova, New York, 1994).
 [13] M. Dion, H. Rydberg, E. Schröder, D. G. Langreth, and B. I. Lundqvist, *Phys. Rev. Lett.* **92**, 246401 (2004).
 [14] G. Román-Pérez and J. M. Soler, *Phys. Rev. Lett.* **103**, 096102 (2009).
 [15] R. D. Mattuk, *A Guide to Feynman Diagrams in the Many-Body Problem* (McGraw-Hill, New York, 1967).
 [16] W. H. Dickhoff and D. Van Neck, *Many-Body Theory Exposed!* (World Scientific, Singapore, 2005).
 [17] C. Barbieri, D. Van Neck and W. H. Dickhoff, *Phys. Rev. A* **76**, 052503 (2007).
 [18] W. H. Dickhoff and C. Barbieri, *Prog. Part. Nucl. Phys.* **52**, 377 (2004).
 [19] C. Barbieri *et al.*, *Phys. Rev. C* **70**, 014606 (2004).
 [20] C. Barbieri, *Phys. Lett. B* **643**, 268 (2006).
 [21] C. Barbieri and M. Hjorth-Jensen, *Phys. Rev. C* **79**, 064313 (2009).
 [22] C. Barbieri, *Phys. Rev. Lett.* **103**, 202502 (2009).
 [23] D. Van Neck, S. Verdonck, G. Bonny, P. W. Ayers, and M. Waroquier, *Phys. Rev. A* **74**, 042501 (2006).
 [24] A. B. Migdal, *Theory of Finite Fermi Systems and Applications to Atomic Nuclei* (John Wiley and Sons, New York, 1967).
 [25] A. L. Fetter and J. D. Walecka, *Quantum Theory of Many-Particle Physics* (McGraw-Hill, New York, 1971).
 [26] L. S. Cederbaum and W. Domke, *Adv. Chem. Phys.* **36**, 205 (1977).
 [27] O. Walter and J. Schirmer, *J. Phys. B: At. Mol. Phys.* **14**, 3805 (1981).
 [28] J. Schirmer, *Phys. Rev. A* **28**, 2395 (1982).
 [29] J. Schirmer, L.S. Cederbaum, and O. Walter, *Phys. Rev. A* **28**, 1237 (1983).
 [30] M. Pernpointner, *J. Chem. Phys.* **121**, 8782 (2004).
 [31] A. B. Trofimov and J. Schirmer, *J. Chem. Phys.* **123**, 144115 (2005).
 [32] A. B. Trofimov, G. Stelter, and J. Schirmer, *J. Chem. Phys.* **117**, 6402 (2002).
 [33] L. Hedin, *Phys. Rev.* **139**, A796 (1965).
 [34] G. Onida, L. Reining, and A. Rubio, *Rev. Mod. Phys.* **74**, 601 (2002).
 [35] F. Aryasetiawan, and O. Gunnarsson, *Rep. Prog. Phys.* **61**, 237 (1998).
 [36] S. Verdonck, D. Van Neck, P. W. Ayers, M. Waroquier, *Phys. Rev. A* **74**, 062503 (2006).
 [37] A. Stan, N. E. Dahlen, and R. van Leeuwen, *J. Chem. Phys.* **130**, 114105 (2009).
 [38] U. von Barth and B. Holm, *Phys. Rev. B* **54**, 8411 (1996);
 [39] B. Holm, *Phys. Rev. Lett.* **83**, 788 (1999).
 [40] E. L. Shirley, *Phys. Rev. B* **54**, 7758 (1996).
 [41] Y. Dewulf, D. Van Neck, and M. Waroquier, *Phys. Rev. B* **71**, 245122 (2005).
 [42] P. Romaniello, S. Guyot, L. Reining, *J. Chem. Phys.* **131**, 154111 (2009).
 [43] S. Boffi, *Nuovo Cimento Lettere* **1**, 931 (1971).
 [44] C. Barbieri and W. H. Dickhoff, *Phys. Rev. C* **63**, 034313 (2001).
 [45] L. D. Faddeev, *Zh. Éksp. Teor. Fiz.* **39** 1459 (1961) [*Sov. Phys. JETP* **12**, 1014 (1961)].
 [46] C. Barbieri and W. H. Dickhoff, *Phys. Rev. C* **68**, 014311 (2003).

- [47] E. R. Davidson, S. A. Hagstrom, S. J. Chakravorty, V. M. Umar, C. F. Fischer, *Phys. Rev. A* **A44**, 7071 (1991).
- [48] S. J. Chakravorty and E. R. Davidson, *J. Phys. Chem.* **100(15)**, 6167 (1996).
- [49] G. Martin, <http://www.weizmann.ac.il/oc/martin/atoms.shtml>
- [50] I. E. McCarthy, R. Pascual, P. Storer, and E. Weigold, *Phys. Rev. A* **40**, 3041 (1989).
- [51] NIST Atomic Spectra Database, NIST Standard Reference Database #78, <http://physics.nist.gov/PhysRefData/ASD/in-dex.html>
- [52] A. Thompson *et al.*, *X-ray Data Booklet* (Lawrence Berkeley National Laboratory, Berkeley, CA, 2001), and references cited therein.
- [53] Degroote *et al.*, to be published.
- [54] The augmented version of the bases (aug-cc-pvXz) were also tested and gave no sizable improvement for the quantities being considered in this work.
- [55] In the ADC language, this means adding fifth-order terms that are introduced at the ADC(5) level.